2009 IEEE International Conference on Robotics and Automation
Kobe International Conference Center
Kobe, Japan, May 12-17, 2009

Design and Implementation of a 9-Axis Inertial Measurement Unit

Pei-Chun Lin and Chi-Wei Ho

Abstract— We report on a 9-axis inertial measurement unit (IMU) which utilizes 3-axis angular velocity measurements from rate gyros and 6-axis linear acceleration measurements from three 2-axis accelerometers. This system is capable of deriving linear acceleration, angular acceleration and angular velocity via simple matrix operations, and it also releases the requirement of accelerometer installation at the center of mass as in the traditional IMU. An optimal configuration of the system is proposed based on the analysis of rigid body dynamics and matrix theory. We performed error analyses, including position, orientation, and sensor noise, and we also report the results of experimental evaluation. We believe the analysis presented in this paper would benefit the practical design of IMUs in the future.

I. INTRODUCTION

For several decades, inertial sensors [1] have been one of the important categories of sensors utilized in various applications, including navigation (robots, vehicles, rockets, and etc) [2], state estimation for motion analysis [3] or dynamic modeling, microsurgery [4], and sports injury avoiding [5]. In modeling dynamics of legged robots, information of external forces, position and orientation states (including their 1st/2nd derivatives) are usually required as essential information for constructing 2nd order dynamic models, and the inertial sensors are appropriate choices to provide some essential information of states. A traditional inertial measurement unit (IMU) is comprised of 3-axis acceleration measurement by accelerometers installed at center of mass (COM) and 3-axis angular velocity measurement by rate gyros. Though full position/orientation state can be reconstructed by models and filter technologies such as the Kalman filter [6], such systems usually yield poor performance and generate unbounded integration error due to their nature of unobservability [7]. Thus, techniques of fusing IMU with other positioning sensors (GPS [8], differential GPS, magnetocompass, and vision system [9]) are widely adapted. While translational displacement, velocity, and acceleration as well as orientation and angular velocity can all be measured by commercially available sensors, the only state left unknown is angular acceleration. Though this information can be derived by differentiation of gyro signals, it is usually noisy. Therefore, in addition to improving the performance of the gyros and associated data acquisition systems, searching for new techniques which are capable of yielding reliable and accurate angular acceleration state plays a nontrivial role in the development of inertial measurement units.

In rigid body dynamics, linear accelerations of any two points on the body, angular acceleration, and angular velocity of the body are related in a specific mathematical equation based on Newton Mechanics (detailed in (1)). Since the linear acceleration and the angular velocity can be measured directly by the accelerometers and the rate gyros, the angular acceleration can readily be derived by utilizing these measurements together with the Newtonic equation. For decades, researchers have tested various methods attempting to recover all three states (totally 9 scalar unknowns) via a minimum set of sensors together with specific computational algorithms, especially in the development of accelerometer-based systems [7], [10]–[12] without utilization of gyros due to various considerations, such as prices, calibration procedure, electronics, and etc. In recent years with the advanced development in micro electrical mechanical systems (MEMS), not only the accelerometers but also multi-axis MEMS rate gyros have become commercially available, low-cost yet with promising performance. All these reasons motivate authors to revisit the question of how to select, place, and orient inertial sensors in order to yield better performance and feasible solutions for practical implementation.

Here, we investigate a 9-axis "advanced IMU" containing 3-axis angular velocity measurements from the rate gyros and 6-axis linear acceleration measurements from the accelerometers at three distinct locations. Comparing to a traditional IMU, this advanced IMU provides instant angular acceleration derivation via linear operation without any differentiation or integration. In addition, the flexible positioning of three 2-axis accelerometers releases the strong constraint of accelerometer installation at COM in the traditional IMU. Moreover, if the accelerometers are capable of 3-axis measurement, the sensor orientation error due to installation can be thoroughly eliminated through a calibration procedure.

Section II introduces the idea of this 9-axis sensory system based on the analysis of rigid body dynamics, followed by Section III which describes the positioning of sensors in detail. Section IV presents the error analysis of the system and briefly describes the calibration procedure. Section V reports the results of experimental evaluation, and Section VI concludes the work.

This work is supported by National Science Council (NSC), Taiwan, under contract NSC 97-2218-E-002-022 and by Tzong Jwo Jang Educational Foundation under contract 97-S-A07.

Authors are with Department of Mechanical Engineering, National Taiwan University, No.1 Roosevelt Rd. Sec.4, Taipei, Taiwan peichunlin@ntu.edu.tw

II. CONSTRUCTION OF SENSING SYSTEM

The acceleration vector, $\mathbf{a}_p$, in an inertial frame $\mathcal{W}$ of a point, p, rigidly attached to an accelerating body frame $\mathcal{B}$ with origin, o, is a function of the body's angular velocity, ω, and angular acceleration, $\dot{\omega}$, as well as the translational acceleration of the body origin, $\mathbf{a}_o$, given by

$$\mathbf{a}_p = \mathbf{a}_o + \dot{\omega} \times \mathbf{r}_{op} + \omega \times (\omega \times \mathbf{r}_{op}), \tag{1}$$

where $\mathbf{r}_{op}$, the fixed position vector of p relative to the body, is presumed known á priori. In general, we are interested in utilizing the measurement from commercially available accelerometers and gyros to derive 9 unknown scalar body states on the right side of the equation, including the COM translational acceleration, $\mathbf{a}_{COM}$, (usually equal to the origin of body frame, $\mathbf{a}_o$), and the angular acceleration and velocity, $\dot{\omega}$ and ω,

$$\begin{array}{rcl} \mathbf{a}_o & := & \mathbf{a}_{COM} = \left[\begin{array}{ccc} a_x & a_y & a_z \end{array} \right]^T \\ \dot{\omega} & = & \left[\begin{array}{ccc} \dot{\omega}_x & \dot{\omega}_y & \dot{\omega}_z \end{array} \right]^T \\ \omega & = & \left[\begin{array}{ccc} \omega_x & \omega_y & \omega_z \end{array} \right]^T. \end{array}$$

The 1-axis rate gyro "fixed" on the body measures the projected angular velocity of spatial body motion, ${}^b\omega_i$, along the sensing direction $\hat{\mathbf{s}}_i$,

$${}^b\omega_i = \omega^T \cdot \hat{\mathbf{s}}_i, \tag{2}$$

where motion is with respect to the inertial frame but the coordinates are represented in the body frame (i.e. letter "b" on the upper left corner of the state). Likewise, the 1-axis accelerometer installed at the point, p, on the body measures the projected linear acceleration in the similar manner,

$${}^b a_j = \mathbf{a}_p \cdot \hat{\mathbf{s}_j} = [\mathbf{a}_o + \dot{\omega} \times \mathbf{r}_{op} + \omega \times (\omega \times \mathbf{r}_{op})] \cdot \hat{\mathbf{s}_j}. \tag{3}$$

Since the position vector, $\mathbf{r}_{op}$, and sensing direction, $\hat{\mathbf{s}_i}$, are invariant with respect to the body frame $\mathcal{B}$, it motivates us to represent the coordinates of dynamic equation (1) in the body frame at every instant while the measured states of the moving rigid body are still with respect to the initial frame:

$${}^b\mathbf{a}_p - {}^b\,\omega \times ({}^b\omega \times {}^b\,\mathbf{r}_{op}) = {}^b\,\mathbf{a}_o + {}^b\,\dot{\omega} \times {}^b\,\mathbf{r}_{op}. \tag{4}$$

In the following content all the equations will be represented in the body coordinates, and notations "b" will be omitted for clear equation presentations. Presumably we have six 1-axis linear acceleration measurements from the accelerometers, $\mathbf{a_m}$, and three 1-axis angular velocity measurements from the rate gyros, $\mathbf{w_m}$,

$$\begin{array}{rcl} \mathbf{a_m} & = & \left[\begin{array}{cccccc} a_1 & a_2 & a_3 & a_4 & a_5 & a_6 \end{array} \right]^T \\ \mathbf{w_m} & = & \left[\begin{array}{ccc} w_1 & w_2 & w_3 \end{array} \right]^T, \end{array}$$

with known sensor positions, $\mathbf{r}_k$, and orientations $\hat{\mathbf{s}_k}$, on the body; the left side of (4) can be computed, and consequently the remaining 6 unknown scalar acceleration states on the right side,

$$\mathbf{x}_{var} := \left[\begin{array}{cc} \mathbf{a}_o & \dot{\omega} \end{array} \right]^T, \tag{5}$$

with respect to the inertial frame can be derived by simple linear computation. This procedure completes the computation of desired body state that we will proceed to detail.

Without loss of generality, we can arrange three 1-axis gyros such that the sensing directions, $\hat{\mathbf{s}_i}$ $_{i=1,2,3}$, align with three principal axes of the body frame, $\hat{\mathbf{s}_1} = \hat{\mathbf{e}_x}, \hat{\mathbf{s}_2} = \hat{\mathbf{e}_y}, \hat{\mathbf{s}_3} = \hat{\mathbf{e}_z}$. In this arrangement, output of the rate gyros readily represents one of the desired body states: angular velocity, $\omega = \mathbf{w_m}$. Similarly, six 1-axis accelerometers can be oriented to measure the linear accelerations, $\mathbf{a_m}$, along the three principal axes of body frame $\mathcal{B}$ as well, each axis with two measurements for symmetrical consideration. Instead of the computation of the inner products described in (2) and (3), computation in the current arrangement of sensing directions only requires the selection of one out of three scalar components of the dynamic equation (4).

Now the question lies in how to place these six 1-axis accelerometers so the remaining unknown state, $\mathbf{x}_{var}$, can be successfully derived. Assuming the locations of six 1-axis accelerometers are defined by six position vectors, $\mathbf{r} = \left[\begin{array}{cccccc} \mathbf{r}_1 & \mathbf{r}_2 & \mathbf{r}_3 & \mathbf{r}_4 & \mathbf{r}_5 & \mathbf{r}_6 \end{array} \right]$, where $\mathbf{r}_j$ behaves the same as $\mathbf{r}_{op}$ defined in (4), and assuming the sensing directions of the sensors are along with $\hat{\mathbf{e}_x}, \hat{\mathbf{e}_y}, \hat{\mathbf{e}_z}, \hat{\mathbf{e}_x}, \hat{\mathbf{e}_y}, \hat{\mathbf{e}_z}$, respectively (as shown in Figure 1(a)), the left side of (4) can readily be computed with sensor measurements $\mathbf{a_m}$ and $\mathbf{w_m}$:

$$\begin{array}{rcl} q_j & := & a_j - (\omega \times (\omega \times \mathbf{r}_j)) \cdot \hat{\mathbf{e}_k} \;\; {\scriptstyle j=1\sim 6 \;\; k=1,2,3,1,2,3} \\ \mathbf{q} & := & \left[\begin{array}{cccccc} q_1 & q_2 & q_3 & q_4 & q_5 & q_6 \end{array} \right]^T \\ & = & \mathbf{a_m} - \mathbf{W}(\mathbf{r})\mathbf{w_{m6}}. \end{array} \tag{6}$$

$\mathbf{W}(\mathbf{r})$ and $\mathbf{w_{m6}}$ are the expanded forms of double cross products between angular velocity and position vectors, in which the gyro measurement, $\mathbf{w_m}$, is represented in the quadratic form, $\mathbf{w_{m6}} = \left[\begin{array}{ccccccc} w_1^2 + w_2^2 & w_1^2 + w_3^2 & w_2^2 + w_3^2 & w_1 w_2 & w_1 w_3 & w_2 w_3 \end{array} \right]^T$. Combining the six scalar equations defined in (4), (5), and (6), the linear system of equations can be represented as $\mathbf{q} = \mathbf{a_m} - \mathbf{W}(\mathbf{r})\mathbf{w_{m6}} = \mathbf{S}(\mathbf{r})\mathbf{x}_{var}$, where $\mathbf{S}(\mathbf{r})$ is the 6×6 matrix,

$$\mathbf{S}(\mathbf{r}) = \left[\begin{array}{cccccc} 1 & 0 & 0 & 0 & r_{1z} & -r_{1y} \\ 0 & 1 & 0 & -r_{2z} & 0 & r_{2x} \\ 0 & 0 & 1 & r_{3y} & -r_{3x} & 0 \\ 1 & 0 & 0 & 0 & r_{4z} & -r_{4y} \\ 0 & 1 & 0 & -r_{5z} & 0 & r_{5x} \\ 0 & 0 & 1 & r_{6y} & -r_{6x} & 0 \end{array} \right]. \tag{7}$$

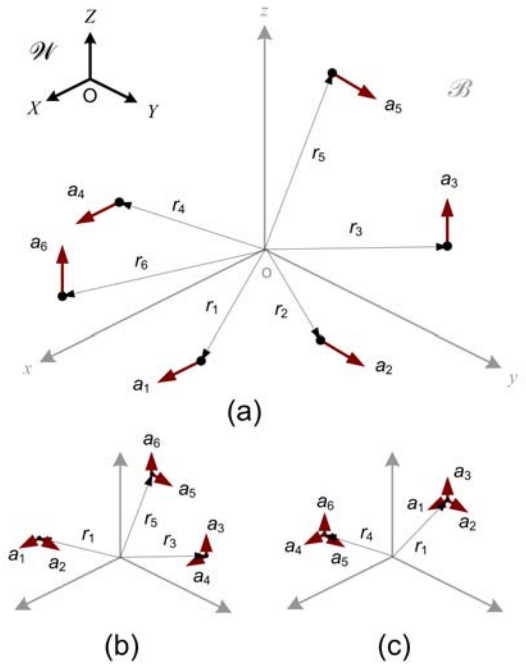

Fig. 1. Three different arrangements of six 1-axis acceleration measurements: (a) Six 1-axis measurements at six distinct locations, (b) Three 2-axis measurements at three distinct locations, (c) Two 3-axis measurements at two distinct locations.

The unknown acceleration states can be derived by the matrix operation

$$\mathbf{x}_{var} = \mathbf{S}(\mathbf{r})^{-1}\mathbf{a_m} - \mathbf{S}(\mathbf{r})^{-1}\mathbf{W}(\mathbf{r})\mathbf{w_{m6}}, \qquad (8)$$

and this equation reveals that the extraction of the desired acceleration data, $\mathbf{x}_{var}$, now hinges upon the rank and numerical condition of the "structure" matrix, $\mathbf{S}(\mathbf{r})$, which is solely a function of positions of accelerometers, $\mathbf{r}$. Since the positions are known á priori and are fixed in the body coordinates, the following task lies on the allocation of accelerometers.

III. SENSOR ALLOCATION

The rise of MEMS sensing technology has yielded commercially available low-cost MEMS accelerometers that have better performance, lower prices, and smaller packaging than those of a decade ago. More importantly, the availability of multi-axis accelerometers[1] significantly simplifies the original complicated electronic and spatial design of multi-sensor systems for multi-axis state measurements. Therefore, the spatial allocations of six 1-axis acceleration measurements presented in this paper can be categorized into three different scenarios: (1) two 3-axis accelerometers (two $\mathbf{r}_j$s) positioned at two distinct locations, (2) three 2-axis accelerometers (three $\mathbf{r}_j$s) positioned at three distinct locations, and (3) six 1-axis accelerometers (six $\mathbf{r}_j$s) positioned at six distinct ocations. We will discuss these cases separately and focus on the invertibility of the structure matrices, $S(\mathbf{r})$, and their numerical conditions detailed as follows.

[1]For example, Analog Devices Inc, Freescale Semiconductor, VTI Technologies, Measurement Specialties Inc/Schaevitz, and STMicroelectronics all produce 3-axis MEMS-based accelerometers.

A. System with two 3-axis Acceleration Measurements

In this scenario six position vectors are combined into two distinct position vectors: $\mathbf{r}_1(=\mathbf{r}_2=\mathbf{r}_3)$ and $\mathbf{r}_4 = (\mathbf{r}_5=\mathbf{r}_6)$, containing measurements of $\{a_1,a_2,a_3\}$ and $\{a_4,a_5,a_6\}$ accordingly as shown in Figure 1(c). The structure matrix, $\mathbf{S}(\mathbf{r})$, is composed of two copies of the dynamic equation (4). For each copy (upper/lower three rows) , the first 3×3 identity matrix the corresponds to the computation of the COM linear acceleration, and the second 3×3 skew-symmetric matrix represents the cross product between the position vector and the angular acceleration vector. Unfortunately, the determinant of the structure matrix, $\mathbf{S}(\mathbf{r})$, is always 0, which indicates that the matrix is not invertible and further implies that the desired acceleration state can't be derived in this configuration. Apparently 6 scalar position variables in $\mathbf{r}_1$ and $\mathbf{r}_4$ are not sufficient to construct six independent vectors in the structure matrix.

B. System with three 2-axis Acceleration Measurements

Following similar logic presented in the previous subsection, the general spatial configuration of a system with three 2-axis acceleration measurements is depicted in Figure 1(b) where three distinct position vectors $\mathbf{r}_1(=\mathbf{r}_2),\mathbf{r}_3(=\mathbf{r}_4),\mathbf{r}_5(=\mathbf{r}_6)$, contain measurements of $\{a_1,a_2\}$, $\{a_3,a_4\}$, and $\{a_5,a_6\}$, respectively. In this scenario, the matrix is composed by three copies of two differently selected scalar components of the spatial dynamic equation (4). The determinant of this 9-variable structure matrix, $\mathbf{S}_{32}(\mathbf{r})$, can be organized as:

$$\begin{aligned} det(\mathbf{S}_{32}(\mathbf{r})) \quad = \quad & -(r1x-r5x)(r5y-r3y)(r3z-r1z) \\ & -(r5x-r3x)(r3y-r1y)(r1z-r5z), \end{aligned} \qquad (9)$$

and this indicates that the arrangement of sensor positions is crucial in order to avoid singularity of the structure matrix. Geometrically, considering a triangle formed by the relative position vectors of sensor positions, the six terms in (9) represent the components of projected vectors of $\mathbf{r}_{13}$, $\mathbf{r}_{35}$, $\mathbf{r}_{51}$ on yz, xy, and zx planes respectively. Various configurations make the determinant of $S_{32}(\mathbf{r})$ zero when the relative positions of accelerometers satisfy the equation (9). For example: when the positions of three sensors have the same x, y, or z components — i.e. the plane composed by the positions of the three sensors (hereafter referred to as the "sensor plane") is parallel to the xy, yz, or zx plane ("sensing plane", the plane spanned by the directions of two sensing vectors). More generally, no matter what orientation of principal axes are, this is also true as long as the sensor plane is parallel to one of three sensing planes.

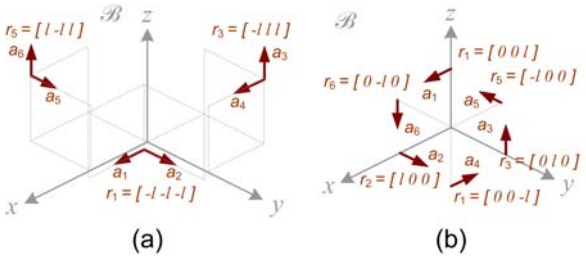

Fig. 2. Configuration of the systems with the best conditioned structure matrices: (a) system with three 2-axis measurements at three distinct locations, (b) system with six 1-axis measurements at six distinct locations.

The condition number defined as the ratio of the largest to the smallest singular values of the matrix further indicates the quality of the inversion. The singular values are determined by high-order polynomials (in the entries of the sensor positions) which is harder to analyze symbolically, yet there is every reason to expect that the condition number is very sensitive to the "shape" and "magnitude" of the sensor positions relative to each other and their locations relative to the COM. Therefore, the general behavior of condition number vs. sensor position can be investigated numerically by moving sensor positions spatially with respect to the current body coordinates. In practice, numerical exploration suggests that the configuration of the three 2-axis accelerometers system shown in Figure 2(a) yields the best condition number 2. Interestingly, because the structure matrix combines entries with and without physical scale both in the same rows — "1" in the first 3×3 identity matrix are dimensionless, and the second 3×3 skew-symmetric matrix has unit of "length" — it turns out there is actually a preferred linear dimension of this system at which the resulting condition number is optimal. For example, a physical installation of sensors with $l = 10cm$ should use "decimeter" as the unit which sets $l = 1$, not centimeter ($l = 10$) or meter ($l = 0.1$) which yield large condition numbers 20 and 10 respectively. The condition number of the matrix is purely determined by the relative magnitudes of its matrix elements; thus, choose a right unit so the magnitudes of the elements close to the optimum condition will reduce the additional error induced by the matrix inversion.

C. System with Six 1-axis Acceleration Measurements

This most general case has been described in Section II and is depicted in Figure 1(a). The structure matrix shown in (7) is a function of 12 scalar position variables. The determinant of structure matrix, $\mathbf{S}(\mathbf{r})$ still contains 16 terms but is not as constructive as $\mathbf{S}_{32}(\mathbf{r})$ shown in Section III-B. Numerical exploration reveals that the configuration shown in Figure 2(b) yields a perfect condition number of 1 when the length scale is 1.

The system in this configuration requires 6 sets of sensor modules positioned on both sides of three principal axes with equal distances, and this increases the complexity of space layout, and both electronic and mechanical designs. In addition, the orientational installation error of each 1-axis accelerometer most likely counteracts the advantage of the perfect structure matrix inversion, keeping noise levels the same. Therefore, in the following sections we focus on the analysis of the system described in the previous Section III-B which requires 3 sets of sensor modules, half in comparison with the current one.

IV. ERROR ANALYSIS AND CALIBRATION

Equation below constructed by importing the best configuration parameters shown in Figure 2(a) into (8) describes the numerical relation between the acceleration outputs and the sensor inputs:

$$\begin{bmatrix} a_x & a_y & a_z & \dot\omega_x & \dot\omega_y & \dot\omega_z \end{bmatrix}^T = \begin{bmatrix} m & 0 & 0 & m & 0 & 0 \\ 0 & m & 0 & 0 & m & 0 \\ 0 & 0 & m & 0 & 0 & m \\ n & n & n & -n & -n & -n \\ -n & -n & n & n & n & -n \\ n & -n & n & -n & n & -n \end{bmatrix} \begin{bmatrix} a_1 \\ a_2 \\ a_3 \\ a_4 \\ a_5 \\ a_6 \end{bmatrix} - \begin{bmatrix} 0 & 0 & 1 & 0 & 0 & 0 \\ 0 & 1 & 0 & 0 & 0 & 0 \\ -1 & 0 & 0 & 0 & 0 & 0 \\ 0 & 0 & 0 & -1 & -1 & 0 \\ 0 & 0 & 0 & 1 & 0 & 1 \\ 0 & 0 & 0 & 0 & -1 & 1 \end{bmatrix} \begin{bmatrix} w_1^2+w_2^2 \\ w_1^2+w_3^2 \\ w_2^2+w_3^2 \\ w_1w_2 \\ w_1w_3 \\ w_2w_3 \end{bmatrix} \quad (10)$$

where $m = 0.5$ and $n = 0.25$. Here, an error analysis is performed to evaluate the effect of each parameter on the final acceleration state. The error equation is defined as follows: $E(X, \Delta e) = |X - X^*|/|X^*|$, where Δe denotes the parameter with small error (or sensor noise), and X and X^* denotes the state of interest and its nominal value, respectively. Since the optimal configuration is symmetric with respect to three principal axes, similar results are expected for all sensing axes. Thus, only analyses of a_x and $\dot\omega_x$ are presented. Higher order terms are ignored.

A. Sensor Noise

The effect of accelerometer noise, Δa_i, and rate gyro noise, Δw_i, on the state a_x and $\dot\omega_x$ are listed below:

$$\begin{aligned}
&E(a_x, \Delta a_i) = \tfrac{\Delta a_i}{a_1+a_4-2(w_2^2+w_3^2)} \ _{i=1,4} \text{ or } = 0 \ _{i=2,3,5,6} \\
&E(a_x, \Delta w_i) = 0 \ _{i=1} \text{ or } \approx \tfrac{4w_i\Delta w_i}{a_1+a_4-2(w_2^2+w_3^2)} \ _{i=2,3} \\
&E(\dot\omega_x, \Delta a_i) = \tfrac{\Delta a_i}{a_1+a_2+a_3-a_4-a_5-a_6+4w_1w_2+4w_1w_3} \ _{i=1,2,3} \\
&E(\dot\omega_x, \Delta a_i) = -\tfrac{\Delta a_i}{a_1+a_2+a_3-a_4-a_5-a_6+4w_1w_2+4w_1w_3} \ _{i=4,5,6} \\
&E(\dot\omega_x, \Delta w_1) = -\tfrac{4(w_2+w_3)\Delta w_1}{a_1+a_2+a_3-a_4-a_5-a_6+4w_1(w_2+w_3)} \\
&E(\dot\omega_x, \Delta w_i) = -\tfrac{4w_1\Delta w_i}{a_1+a_2+a_3-a_4-a_5-a_6+4w_1(w_2+w_3)} \ _{i=2,3}
\end{aligned}$$

The trend matches the system configuration (or formulation of (10)) which reveals that: (1) linear acceleration

at the COM is only affected by the accelerometer measurements whose sensing directions are parallel to those specific motion directions. Thus, only sensor noise Δa_1 and Δa_4 have impacts on the state a_x as shown in the first two equations. Contrarily, angular velocity has opposite effects as shown in the 3rd and 4th equations. (2) Since the positions of all three 2-axis accelerometers have equal position offsets with respect to all three principal axes in the current configuration, measured body angular acceleration is affected by all accelerometer measurements with equal significance as shown in the 5th and 6th equations. In addition, the small coefficients in these equations also confirm that the structure matrix is well-conditioned — the variations of sensor noises do not alter estimated state significantly.

B. Accelerometer Positioning Error

The effect of accelerometer positioning error, $\Delta r_{ij\ \ i=1,2,3,4,5,6;j=x,y,z}$, on the state a_x and $\dot{\omega}_x$ are listed below:

$$
\begin{aligned}
&E(a_x, \Delta r_{5x}) = E(a_x, \Delta r_{5y}) = E(a_x, \Delta r_{5z}) = 0 \\
&E(a_x, \Delta r_{ix}) = \tfrac{(w_2^2+w_3^2)\Delta r_{ix}}{a_1+a_4-2(w_2^2+w_3^2)} \ \ i=1,3 \\
&E(a_x, \Delta r_{iy}) \\
&\approx \tfrac{a_1-a_2+a_3-a_4+a_5-a_6-4(w_1w_2-w_1w_3+w_2w_3)\Delta r_{iy}}{4(a_1+a_4-2(w_2^2+w_3^2))} \ \ i=1,3 \\
&E(\dot{\omega}_x, \Delta r_{5x}) \\
&\approx \tfrac{(a_1-a_4+4w_1w_2+4w_1w_3)\Delta r_{5x}}{2(a_1+a_2+a_3-a_4-a_5-a_6+4w_1w_2+4w_1w_3)} \\
&E(\dot{\omega}_x, \Delta r_{1x}) \\
&\approx \tfrac{(-a_1+a_2-a_3+a_4-a_5+a_6-4w_1w_2-4w_1w_3+4w_2w_3+4w_2^2+4w_3^2)\Delta r_{1x}}{4(a_1+a_2+a_3-a_4-a_5-a_6+4w_1w_2+4w_1w_3)}
\end{aligned}
$$

The position vector $\mathbf{r}_5$ doesn't have any effect on a_x since the accelerometer with this position vector doesn't have any sensing direction along with the x direction as shown in Figure 2(a) or (10). $\Delta r_{ix\ \ i=1,3}$ affects a_x through angular velocity terms, but not through a_1 and a_4 since the sensing direction is parallel to the direction of error. Only positioning errors perpendicular to the x-axis affect the measurement of a_x from all sensors, and they are equally significant due to equal position offsets with respect to the principal axes. Effect of Δr_{ix} and $\Delta r_{iz\ \ i=1,3}$ on a_x have similar formulations so the presentation of the later one is omitted. Angular acceleration, $\dot{\omega}_x$, is determined by all sensor measurements shown in (10); thus the analysis is presented in much more complicated. The error in r_{5x}, r_{3y}, and r_{1z} have similar effect because the error directions are perpendicular to the sensing directions, and the the presentation of the later two are omitted. The error in the remaining six directions $(r_{1x}, r_{1y}, r_{3x}, r_{3z}, r_{5y}, r_{5z})$ also have similar effects on $\dot{\omega}_x$ due to symmetric reason, so only $E(\dot{\omega}_x, \Delta r_{1x})$ is presented.

If the actual body configuration doesn't allow symmetric sensor installation the same as the best situation shown Figure 2(a), a new structure matrix and its inverse can be recalculated. Thus, the positioning error here specifically refer to the resolution of installation error, not including the error due to unsymmetrical positioning.

C. Accelerometer Orientation Error and Calibration

If the sensing directions of the sensors do not not align perfectly with their assigned directions (here, the principal axes), the sensors will response to the accelerations in other axes, which cause severe state reconstruction errors, especially when the accelerations in different principal axes varying significantly with time. Since the MEMS 3-axis accelerometers are widely available with comparable cost to the 2-axis accelerometers, the feasible solution to this problem due to installation error is to use 3-axis accelerometers and to perform a 3-dimensional calibration procedure briefly described as follows. Assuming the 3-axis measurements in the MEMS accelerometers are mutually orthogonal to each other, the relation of these axes to the principal axes of the body frame is a rotation matrix. The parameters of the matrix can be found by performing a 3-dimensional rotation of the system: first, align the principal axes of the system to those of the world frame. Second, rotate the system slowly along with three principal axes of the world frame sequentially; in the meantime collect data of sensor measurements and actual body orientation in order to yield acceleration due to gravity. Then perform the least square technique to find the parameters.

V. EXPERIMENT RESULTS

A benchtop apparatus with one controllable rotational degree of freedom was utilized for experimental evaluation of the proposed system. The required measurements of three 2-axis accelerations and one 3-axis angular velocity of the IMU system were measured by three 3-axis accelerometers (ADXL330, Analog Device) and two 2-axis rate gyros (IDG-300, InvenSense), respectively. An additional 3-axis accelerometer was also mounted at the COM for performance comparison. Data were collected by a real-time embedded control system (sbRIO-9632, National Instruments) running at 1KHz. The COM of the IMU system was positioned on the rotating apparatus with designated distance, and the apparatus was driven in a sinusoidal motion under PID position control. Thus, the COM was subjected to tangential, normal, and angular accelerations. In current measurements, direction of the rotating axis is parallel to that of the gravity, so the gravity induced acceleration does not affect the measurements. Further 3-dimensional accelerating tests will be perform after the IMU system is fused with orientation sensors which can remove gravity effectively from the accelerometer measurements.

Figure 3 plots the theoretical estimated and experimental measured body states. Because of position control and unavoidable apparatus vibration during varying-speed rotating motion, the experimentally measured states introduce slightly time delay and measurement noises as opposed to the smooth sinusoidal curves derived

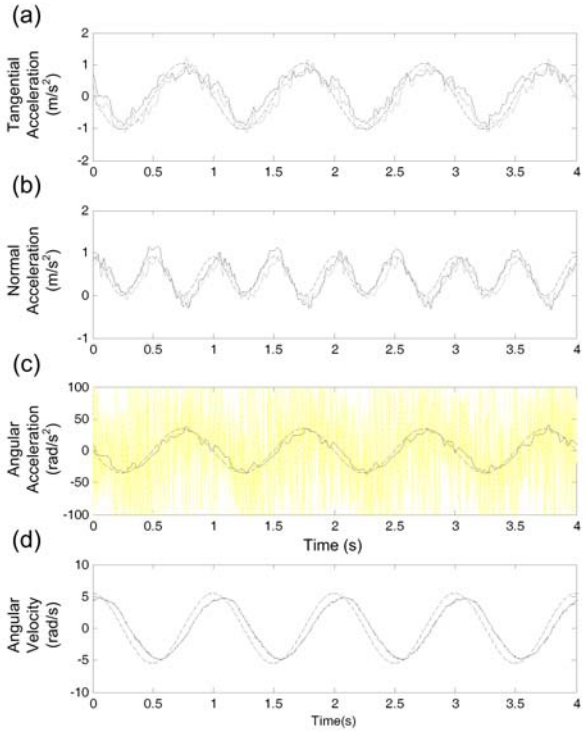

Fig. 3. Plots of theoretical estimated (dashed lines) and experimental measured body states (solid lines: the 9-axis IMU; dotted lines: the traditional IMU). (a),(b),(c),(d) denote tangential acceleration, normal acceleration, angular acceleration, and angular velocity respectively.

in the theoretical calculations, but all states deliver correct measurements in the sense of magnitudes and trends. The 9-axis IMU system delivers comparable measurement of the linear acceleration at COM in comparison with that from the traditional IMU which has measurements directly at the designated location. This indicates that one of the merit of the 9-axis IMU system can indeed be achieved — releasing the requirement of direct acceleration measurement at the COM as in the traditional IMU. In addition, while the traditional IMU can only derive noisy angular acceleration by differentiation of the angular velocity measurement, the 9-axis IMU system deliver the nice measurement. This confirms the second merit of the 9-axis IMU — the angular acceleration can be yielded via simple computation as proposed in the previous sections.

VI. CONCLUSIONS AND FUTURE WORKS

We have investigated a 9-axis "advanced IMU" which utilizes 3-axis angular velocity measurement from rate gyros and 6-axis linear acceleration measurement from three 2-axis accelerometers. Design of this sensory system was based on the analysis of rigid body dynamics and matrix theory, and an optimal configuration of the system with three 2-axis accelerometers was proposed. The experimental results confirmed that though the sensors of the 9-axis IMU do not located at the COM, it is capable of delivering comparable linear acceleration measurement in comparison with the traditional IMU. In addition, it yields correct angular acceleration as the equation predicts. We also performed error analyses of the optimized system, including positioning, orientation, and sensor noise.

Currently we are in the process of testing the system in reality under various different accelerating conditions. In the meantime, we are searching for suitable position and orientation sensors to be fused with the proposed IMU system, thus to construct an observable system capable of accurate full body state estimation for analysis of dynamic locomotion in the legged robots.

VII. ACKNOWLEDGMENTS

This work is supported by National Science Council (NSC), Taiwan, under contract NSC 97-2218-E-002-022 and by Tzong Jwo Jang Educational Foundation under contract 97-S-A07.

References

[1] N. Barbour and G. Schmidt, "Inertial sensor technology trends," IEEE Sensors Journal, vol. 1, no. 4, pp. 332–339, 2001.

[2] J. L. Weston and D. H. Titterton, "Modern inertial navigation technology and its application," IEEE Electronics and Communication Engineering Journal, vol. 12, no. 3, pp. 49–64, 2000.

[3] D. Giansanti, V. Macellari, G. Maccioni, and A. Cappozzo, "Is it feasible to reconstruct body segment 3-d position and orientation using accelerometric data?" IEEE Transactions on Biomedical Engineering, vol. 50, no. 4, pp. 476–483, 2003.

[4] W. T. Ang, P. K. Khosla, and C. N. Riviere, "Nonlinear regression model of a low-g mems accelerometer," IEEE Sensors Journal, vol. 7, no. 1, pp. 81–88, 2007.

[5] J. J. Crisco, J. J. Chu, and R. M. Greenwald, "An algorithm for estimating acceleration magnitude and impact location using multiple nonorthogonal single-axis accelerometers," Journal of Biomechanical Engineering, vol. 126, no. 6, pp. 849–854, 2004.

[6] R. E. Kalman, "A new approach to linear filtering and prediction problems," Transactions of the ASME – Journal of Basic Engineering, vol. 82, no. Series D, pp. 35–45, 1960.

[7] P. Lin and H. Komsuoglu and D. E. Koditschek, "Sensor data fusion for body state estimation in a hexapod robot with dynamical gaits," IEEE Transactions on Robotics, vol. 22, no. 5, pp. 932–943, 2006.

[8] D. T. Knight, "Rapid development of tightly-coupled gps/ins systems," IEEE AES Systems Magazine, vol. 12, no. 2, pp. 14–18, Feb 1997.

[9] S. I. Roumeliotis, A. E. Johnson, and J. F. Montgomery, "Augmenting inertial navigation with image-based motion estimation," in IEEE International Conference on Robotics and Automation, 2002.

[10] A. J. Padgaonkar, K. W. Krieger, and A. I. King, "Measurement of angular accelerarion of a rigid body using linear accelerometers," Transactions of the ASME, vol. 42, pp. 552–556, 1975.

[11] J. Chen, S. Lee, and D. B. DeBra, "Gyroscope free strapdown inertial measurement unit by six linear accelerometers," Journal of Guidance, Control, and Dynamics, vol. 17, no. 2, pp. 286–290, 1994.

[12] K. Parsa, T. A. Lasky, and B. Ravani, "Design and implementation of a mechatronic, all-accelerometer inertial measurement unit," IEEE/ASME Transactions on Mechatronics, vol. 12, no. 6, pp. 640–650, 2007.